J. Microbiol. Biotechnol. (2013), 23(9), 1287–1292
http://dx.doi.org/10.4014/jmb.1304.04047

jmb

Biosynthesis of Silver Nanoparticles by Phytopathogen *Xanthomonas oryzae* pv. *oryzae* Strain BXO8

Kannan Badri Narayanan[1,2] and Natarajan Sakthivel[1]*

[1]*Department of Biotechnology, School of Life Sciences, Pondicherry University, Kalapet, Puducherry 605 014, India*
[2]*School of Biotechnology, Graduate School of Biochemistry, and Research Institute of Protein Sensor, Yeungnam University, Gyeongsan 712-749, Republic of Korea*

Received: April 17, 2013
Revised: June 3, 2013
Accepted: June 7, 2013

First published online
June 10, 2013

**Corresponding author*
Phone: +91-413-2654430;
Fax: +91-413-2655255;
E-mail: puns2005@gmail.com

pISSN 1017-7825, eISSN 1738-8872

Extracellular biogenic synthesis of silver nanoparticles with various shapes using the rice bacterial blight bacterium *Xanthomonas oryzae* pv. *oryzae* BXO8 is reported. The synthesized silver nanoparticles were characterized by UV-Vis spectroscopy, powder X-ray diffractometry (XRD), scanning electron microscopy, energy dispersive X-ray spectrometry, and high-resolution transmission electron microscopy (HR-TEM). Based on the evidence of HR-TEM, the synthesized particles were found to be spherical, with anisotropic structures such as triangles and rods, with an average size of 14.86 nm. The crystalline nature of silver nanoparticles was evident from the bright circular spots in the SAED pattern, clear lattice fringes in the high-resolution TEM images, and peaks in the XRD pattern. The FTIR spectrum showed that biomolecules containing amide and carboxylate groups are involved in the reduction and stabilization of the silver nanoparticles. Using such a biological method for the synthesis of silver nanoparticles is a simple, viable, cost-effective, and environmentally friendly process, which can be used in antimicrobial therapy.

Keywords: Bacterium, *Xanthomonas oryzae* pv. *oryzae*, silver nanoparticles, UV-Vis spectroscopy, electron microscopy

Introduction

In recent times, advancements in the field of nanobiotechnology linking biological sciences to nanosciences for tailoring of materials at the atomic level has aided in attaining the unique chemical, optical, magnetic, mechanical, and electrical magnetic properties for harnessing the benefits in environmental and biomedical fields [22]. The synthesis of nanoparticles and their self-assembly is a cornerstone of nanobiotechnology owing to its cost-effective and environmentally benign methodologies. Despite several rapid and hazardous chemical methodologies, increasing awareness towards green chemistry and other biological processes has led to a desire to develop an eco-friendly approach for the synthesis of environmentally benevolent nanoparticles using microorganisms. It has been well documented that many microbes can detoxify toxic metal ions from soils and solutions by bioreduction into nontoxic insoluble metal nanoclusters.

Several microorganisms are involved in the accumulation of heavy metals from ore mines and runoffs in order to clean up the polluted site. Klaus *et al*. [7] were the first to report a silver mine bacterium, *Pseudomonas stutzeri* AG259, which intracellularly accumulated silver nanoparticles with size up to 200 nm in periplasmic space. Similarly, *Corynebacterium* sp. [23], *Bacillus* sp. [17], and *Lactobacillus* sp. [12] produced intracellular silver nanoparticles. However, extracellular synthesis of silver nanoparticles deserves merit due to its easy downstream processing and its applications. Biologically synthesized silver nanoparticles have enormous applications as intercalating material for electrical batteries, as optical receptors, homogeneous/heterogeneous catalysts in chemical reactions, antimicrobial agents, spectrally selected coatings for solar energy

absorption, optical sensors in optoelectronics, and biolabelling in biomedical industry [13, 19]. Extracellular synthesis of silver nanoparticles was reported in *Aeromonas* sp. [2], *Morganella* sp. [16], *Geobactersulfurreducens* [8], *B. cereus* [20], and *Stenotrophomonas maltophilia* [15]. Even the culture supernatants of the Enterobacteriaceae (*Klebsiella pneumonia*, *Enterobacter cloacae*, *Escherichia coli*) and *B. licheniformis* showed formation of silver nanoparticles by reduction of Ag^{+} to Ag^{0}. It is believed that nitroreductase enzymes may be involved in the silver ion reduction process [6, 18]. Therefore, the potential of microorganisms and its enzymes have received importance for the synthesis of silver nanoparticles by the green chemistry approach without use of any toxic chemicals, high pressure, energy and temperature [14].

A myriad of bioreducing agents are available from various biological organisms for the reduction of silver ions. All these agents influence the morphology and dispersity of the nanoparticles in solution and its optoelectronic and physicochemical properties. By exploring the bioreducing and stabilizing agents, the nanoparticles of well-defined size and morphology can be modulated in accordance to its applications. *Xanthomonas oryzae* pv. *oryzae* is a phytopathogenic bacterium belonging to the family Pseudomonadaceae, which causes bacterial blight of rice. Herein, we report on the biogenic extracellular synthesis of silver nanoparticles by a phytopathogenic bacterium, *X. oryzae* pv. *oryzae* BXO8.

Materials and Methods

Materials

All chemicals used were of analytical grade purchased from Himedia Laboratories Pvt. Ltd., India. *Xanthomonas oryzae* pv. *oryzae* BXO8 was obtained from the Centre for Cellular and Molecular Biology (CCMB), India. Experiments were done in triplicates and the results obtained were analyzed using Origin Pro 8.0 SRO software (OriginLab Corporation, USA).

Extracellular Synthesis of Silver Nanoparticles by *X. oryzae* pv. *oryzae* BXO8

X. oryzae pv. *oryzae* BXO8 (0.6 OD) was inoculated into 100 ml of nutrient broth in an Erlenmeyer flask and incubated at 28°C, 180 rpm for 36 h. The culture was then centrifuged at 1,000 ×*g* for 10 min and 10 g of biomass was inoculated into 100 ml of aqueous solution containing 10^{-3} M silver nitrate and incubated at 28°C, 180 rpm for 72 h. The formation of silver nanoparticles was monitored using a UV-Vis spectrophotometer.

Characterization of Biogenic Silver Nanoparticles by *X. oryzae* pv. *oryzae* BXO8

UV-Vis spectrophotometric analysis. The color change was monitored in the silver nitrate solution incubated with bacterial biomass and the aliquots of the reaction solution were sampled periodically. The UV-Vis spectra were measured in 10 mm optical-path-length quartz cuvettes in a UV-Vis spectrophotometer (Amersham Biosciences; Model: Ultrospec 2100 pro).

Powder X-Ray Diffraction Studies

The aqueous silver nanoparticles were drop-coated onto glass substrate and powder X-ray diffraction (XRD) measurements were carried out on a PANalyticalX'pert PRO X-ray diffractometer (The Netherlands). The size of silver nanoparticles was calculated through Debye-Scherer's equation: $L = (0.94\lambda)/(B \cos \theta)$, where L is the average crystal size, λ is the X-ray wavelength (λ = 1.5406 Å), θ is Bragg's angle (2θ), and B is the full-width at half-maximum (FWHM) in radians [3].

Scanning Electron Microscopy and Energy Dispersive X-Ray Spectrometry

The silver nanoparticles were mounted onto copper stubs and the images were studied using scanning electron microscopy (SEM) (HITACHI; Model: S-3400N) with secondary electron detectors at an operating voltage of 20 kV. For elemental analysis, energy dispersive X-ray spectrometry (EDS) was done in a Noran-System Six X-ray microanalysis system (Thermo Electron Corporation, USA).

Fourier Transform Infra-Red (FTIR) Spectroscopy and Sodium Dodecyl Sulphate-Polyacrylamide Gel Electrophoresis

FTIR measurement was performed by grinding the washed samples of silver nanoparticles with KBr and pressed into thin pellets. The spectrum was recorded on a Thermo Nicolet (model 6700) instrument in the diffuse transmittance mode operating at a resolution of 4 cm^{-1} over 4,000–500 cm^{-1}. To analyze the bacterial proteins capped on the silver nanoparticles synthesized by *X. oryzae* pv. *oryzae* BXO8, the silver nanoparticles were centrifuged at 25,000 ×*g* for 15 min and the pelleted nanoparticles were washed thrice in sterile deionized water to eliminate the unbound proteins from the nanoparticles. These nanoparticles capped with proteins were dissolved in SDS gel-loading buffer and denatured at 90°C for 10 min, and electrophoresed by 12% sodium dodecyl sulfate-polyacrylamide gel electrophoresis (SDS-PAGE). The resolved protein bands were visualized by silver staining [14].

Thermogravimetric Analysis (TGA)

A known quantity of silver nanoparticles coated with biological material was subjected to TGA (TA Instruments; Model: Q600 SDT) in a platinum crucible at a heating rate of 10°C/min under an inert atmosphere of nitrogen.

High-Resolution Transmission Electron Microscopy (HR-TEM)

The size and morphology of biogenic silver nanoparticles were determined by high-resolution TEM. Samples for high-resolution TEM analysis were prepared on carbon-coated copper grids. The films on the grids were measured on a JEOL model

3010 microscope operated at an accelerating voltage of 200 keV with a wavelength (λ) of 0.0251 Å.

Results and Discussion

UV-Vis spectroscopy determines the stability and dispersity of metal nanoparticles in aqueous solution.The experimental flask incubated with bacterial biomass was observed with change of color to yellowish-brown with the surface plasmon resonance (SPR) band centered at 415 nm after 72 h, due to the collective oscillations of conduction electrons of silver nanoparticles (Fig. 1). In the control flask with silver nitrate alone, no color change was observed. Mie theory explains that the shape, and position of the SPR band have been influenced by the size, shape, and monodispersity of the nanoparticles [10, 21]. Powder XRD was used to solve the crystal structure, including their lattice constants, and geometry and identification of materials. XRD analysis of the nanoparticles showed intense peaks of Bragg's reflection corresponding to (111), (200), (220), and (311) at 2θ values of 38.09°, 46.25°, 67.49°, and 76.87° based on the fcc structure of silver, which were in good agreement with reference to the unit cell of the fcc structure of metallic silver (JCPDS File No. 00-003-0931) with a lattice parameter of a = 4.06 Å and with a space group of Fm-3m (Fig. 2). The mean size of silver nanoparticles was calculated using the Debye-Scherer's equation by determining the width of the (200) Bragg's reflection. The size of the nanoparticles was thus determined to be about 12.67 nm

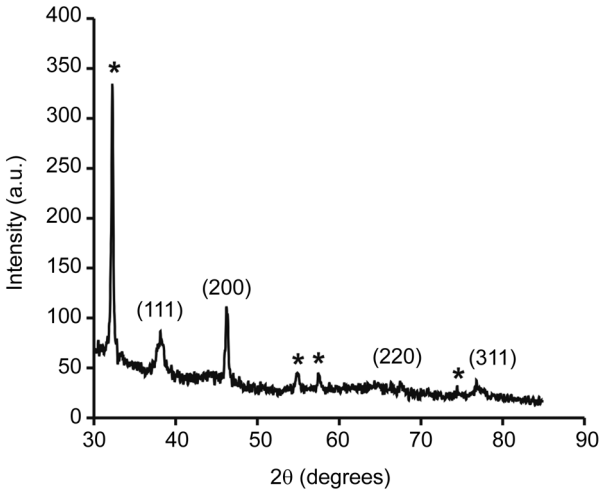

Fig. 2. XRD pattern of silver nanoparticles by produced *X. oryzae* pv. *oryzae* BXO8.
The principal Bragg reflections are identified. The strong peak (*) is due to the formation of amorphous/nano crystals of macromolecules.

for silver nanoparticles, which was in fairly good agreement with the nanoparticles size estimated by TEM analysis. The Bragg's reflections of (111), (220), and (311) were considerably weak and broadened relative to the intense (200) reflection. This indicated that the silver nanocrystals were predominantly (200)-oriented. The spot-profile EDS of silver nanoparticles showed strong signals for silver atoms, along with weak

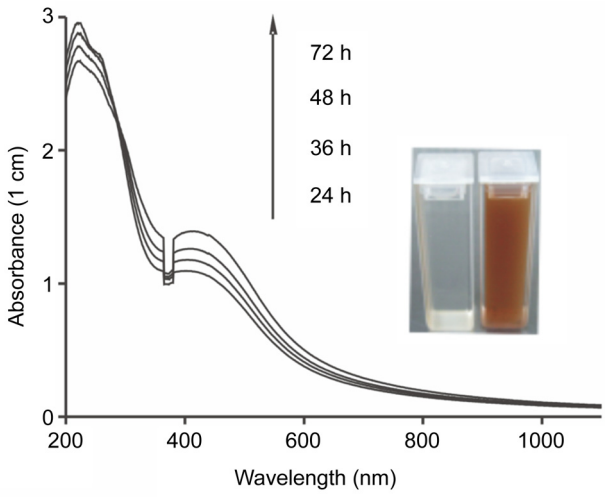

Fig. 1. UV-Vis spectra as a function of time of the reaction of aqueous solution of *X. oryzae* pv. *oryzae* BXO8 with 10^{-3} mol/l $AgNO_3$.

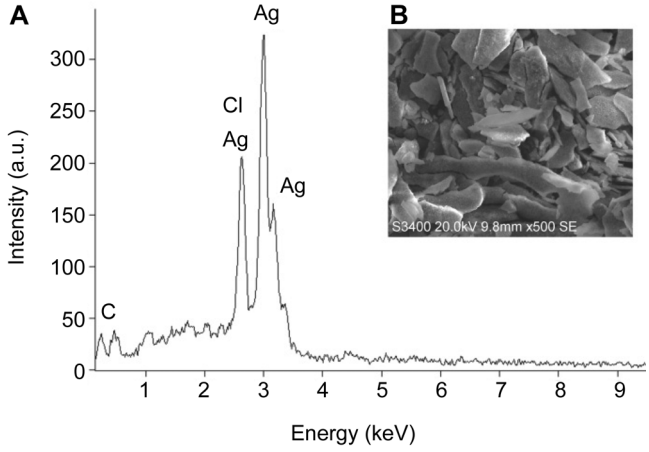

Fig. 3. Characterization of silver nanoparticles produced by *X. oryzae* pv. *oryzae*
(**A**) EDS profile of silver nanoparticles from aqueous solution of *X. oryzae* pv. *oryzae* BXO8 showing silver peaks at 3.01 keV and chlorine peak at 2.96 keV. (**B**) SEM image of silver nanoparticles at a magnification of 40k×.

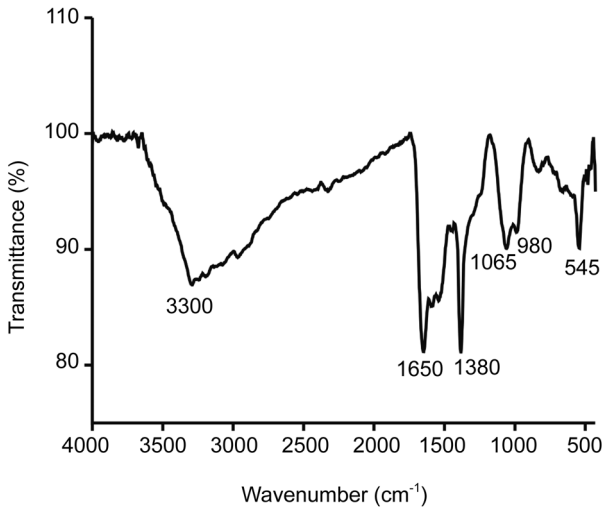

Fig. 4. FTIR spectrum of silver nanoparticles produced by *X. oryzae* pv. *oryzae* BXO8.

signals from carbon and chlorine (Fig. 3A). These weak signals could have arisen from X-ray emission from macromolecules like proteins/enzymes or other organic components bound to the nanoparticles or in the vicinity of the particles. SEM analysis showed asymmetrical distribution of biogenic silver particles at a magnification of 40k× (Fig. 3B). The FTIR spectrum showed bands at 3,300, 1,650, 1,380, and 1,065 cm^{-1}. The band at 3,300 cm^{-1} was identified as H-bonded in –OH stretching. The peak at 1,650 cm^{-1} was due to C=O stretch in the amide I band. The strong peak at 1,380 cm^{-1} was due to the symmetric stretching of the carboxylate anion (COO^-) and the peak at 1,065 cm^{-1} was due to C–OH stretching in primary alcohols (Fig. 4). Balaji *et al*. [1] reported that the carbonyl group (C=O) from amino acid residues and peptides has the stronger ability to bind silver ion. These observations indicate that the presence of protein molecules on the surface of the silver nanoparticles is involved in stabilization. SDS-PAGE results showed that the protein band with the molecular mass of ~70 kDa was capping and stabilizing the silver nanoparticles synthesized by *X. oryzae* pv. *oryzae* BXO8 (Fig. 5). The TGA plot of silver nanoparticles showed an initial weight loss due to water molecules up to 100°C and thereafter a steady weight loss until 700°C accounting for ~40% of the sample weight, due to the desorption of bioorganic components on the nanoparticles secreted by *X. oryzae* pv. *oryzae* BXO8 (Fig. 6).

The size and morphology of silver nanoparticles were determined by TEM. The representative silver nanoparticles produced by *X. oryzae* pv. *oryzae* BXO8 were deposited on lacey carbon-coated copper 200-mesh grids and the morphology of the nanoparticles was found to be spherical with anisotropic structures such as triangles and rods in the range of 3.06–74.16 nm, with an average size of 14.86 nm at a magnification of 50k×, and the particles were stable for a month at room temperature (Figs. 7 and 8). The spherical nanoparticles showed (200) orientation with the top surface normal to the electron beam, with the lattice spacing of 0.205 nm at a magnification of 800k×. The ability to modulate the shape of nanoparticles by the microorganism

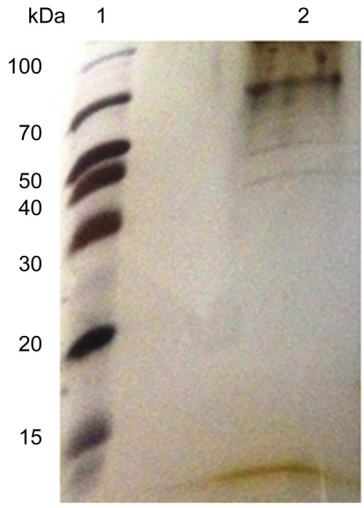

Fig. 5. SDS-PAGE analysis of proteins capped on the silver nanoparticles synthesized by *X. oryzae* pv. *oryzae* BXO8.
Lane 1, protein molecular mass markers; lane 2, silver nanoparticles.

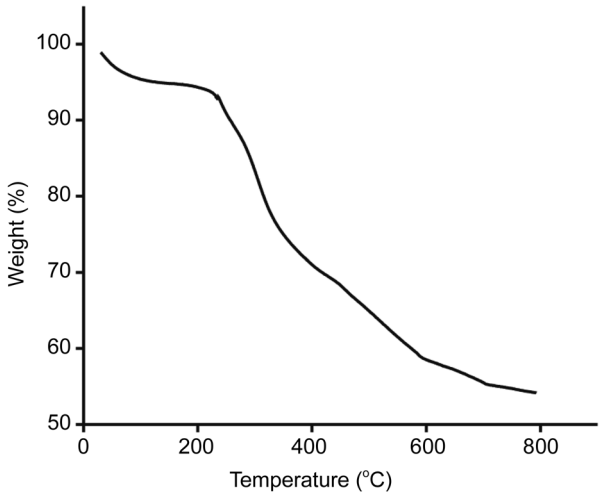

Fig. 6. Thermogravimetric analysis of silver nanoparticles by *X. oryzae* pv. *oryzae* BXO8.

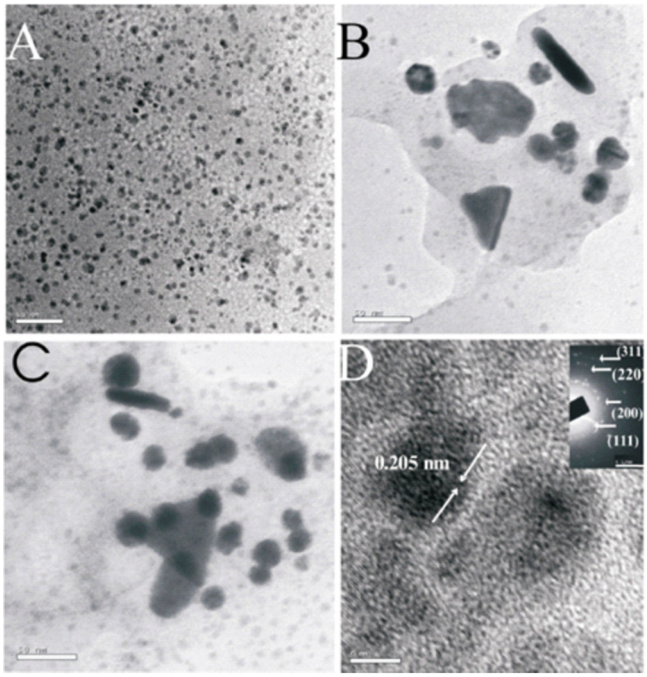

Fig. 7. TEM micrograph of silver nanoparticles.
(**A**–**C**) Representative TEM images of silver nanoparticles by *X. oryzae* pv. *oryzae* BXO8. (**D**) Spherical particle showing the lines traversing the entire particle are the pores as viewed perpendicular to the pore axis. The inset of (**D**) is the SAED pattern of the nanoparticles showing the rings arisen due to the reflections from (111), (200), (220), and (311).

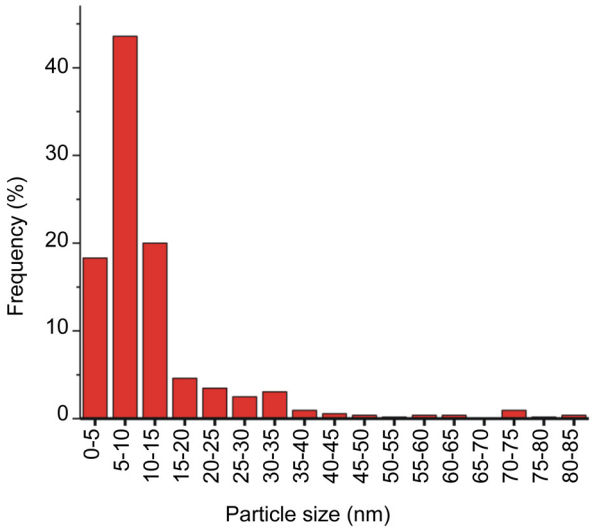

Fig. 8. Histogram of distribution of silver nanoparticles produced by *X. oryzae* pv. *oryzae* BXO8.

opens up an exciting possibility to explore further microbial sources. The SAED pattern with bright circular rings corresponding to (111), (200), (220), and (311) planes exhibited the crystallinity of nanoparticles (Fig. 7D). Although silver is toxic to bacteria, it exhibits a special detoxification system by expressing small periplasmic silver-binding proteins, which bind silver at the cell surface, and by efflux pumps propulsions of metals from the cytoplasm [3, 9]. It is generally believed that an organic matrix containing silver-binding protein acts as nucleation centers for the formation of silver nanoparticles. Naik *et al*. [11] showed that silver-precipitating peptides (AG3 and AG4) have the potential to form fcc structured silver crystals from aqueous solution of silver ions. In *Bacillus* sp. the secretion of cofactor NADH and NADH-dependent enzymes-especially nitrate reductase, was responsible for the bioreduction of silver ions to silver nanoparticles [5].

In summary, the extracellular synthesis of silver nanoparticles using the phytopathogenic bacterium *X. oryzae* pv. *oryzae* BXO8 has been demonstrated. The nanoparticles were characterized by UV-Vis, XRD, FTIR, SEM, EDS, and HR-TEM measurements. The crystalline nature of the silver nanoparticles was evident from the bright circular spots in the SAED pattern, clear lattice fringes in the high-resolution TEM images, and the peaks in the XRD pattern. The FTIR spectrum showed that biomolecules containing amide and carboxylate groups are involved in the reduction and stabilization of the silver nanoparticles. Thus, the ability of the bacterium to modulate the shape of nanoparticles opens up the exciting possibility to explore further microbial sources for various applications in antimicrobial therapy.

Acknowledgments

The financial support from the Council of Scientific and Industrial Research (CSIR), New Delhi, India, is gratefully acknowledged.

References

1. Balaji D, Basavaraja S, Deshpande S, Bedre R, Mahesh D, Prabhakar BK, *et al*. 2009. Extracellular biosynthesis of functionalized silver nanoparticles by strains of *Cladosporium cladosporioides*. *Colloids Surf. B Biointerfaces* **68:** 88-92.
2. Fu MX, Li QB, Sun DH, Lu YH, he N, Deng X, *et al*. 2006. Rapid preparation process of silver nanoparticles by bioreduction and their characterizations. *Chin. J. Chem. Eng.* **14:** 114-117.
3. Gupta A, Silver S. 1998. Molecular genetics: silver as a biocide: will resistance become a problem? *Nat. Biotechnol.* **16:** 888.

4. Holzwarth U, Gibson N. 2011. The Scherrer equation versus the 'Debye-Scherrer equation'. *Nat. Nanotechnol.* **6:** 534.
5. Kalimuthu K, Babu RS, Venkataraman D, Mohd B, Gurunathan S. 2008. Biosynthesis of silver nanocrystals by *Bacillus licheniformis*. *Colloids Surf. B Biointerfaces* **65:** 150-153.
6. Kalishwaralal K, Deepak V, Ramakumarpandian S, Nellaiah H, Sangiliyandi G. 2008. Extracellular biosynthesis of silver nanoparticles by the culture supernatant of *Bacillus licheniformis*. *Mat. Lett.* **62:** 4411-4413.
7. Klaus T, Joerger R, Olsson E, Granqvist CG. 1999. Silver based crystalline nanoparticles, microbially fabricated. *Proc. Natl. Acad. Sci. USA* **96:** 13611-13614.
8. Law N, Ansari S, Livens FR, Renshaw JC, Lloyd JR. 2008. The formation of nano-scale elemental silver particles *via* enzymatic reduction by *Geobacter sulfurreducens*. *Appl. Environ. Microbiol.* **4:** 7090-7093.
9. Li XZ, Nikaido H, Williams KE. 1997. Silver-resistant mutants of *Escherichia coli* display active efflux of Ag^{+} and are deficient in porins. *J. Bacteriol.* **179:** 6127-6132.
10. Mie G. 1908. "Beitrage zer optik truber meiden speziell kolloidaler metallosungen." *Ann. Phys. (Leipzig)* **25:** 377-445.
11. Naik RR, Stringer SJ, Agarwal G, Jones SE, Stone MO. 2002. Biomimetic synthesis and patterning of silver nanoparticles. *Nat. Mater.* **1:** 169-172.
12. Nair B, Pradeep T. 2002. Coalescence of nanoclusters and formation of submicron crystallites assisted by *Lactobacillus* strains. *Cryst. Growth Des.* **2:** 293-298.
13. Narayanan KB, Sakthivel N. 2011. Heterogeneous catalytic reduction of anthropogenic pollutant, 4-nitrophenol by silver-bionanocomposite using *Cylindrocladium floridanum*. *Bioresour. Technol.* **102:** 10737-10740.
14. Narayanan KB, Sakthivel N. 2011. Facile green synthesis of gold nanostructures by NADPH-dependent enzyme from the extract of *Sclerotiumrolfsii*. *Colloids Surf. A Physicochem. Eng. Asp.* **380:** 156-161.
15. Oves M, Khan MS, Zaidi A, Ahmed AS, Ahmed F, Ahmad E, *et al*. 2013. Antibacterial and cytotoxic efficacy of extracellular silver nanoparticles biofabricated from chromium reducing novel OS4 strain of *Stenotrophomonas maltophilia*. *PLoS One* **8:** e59140.
16. Parikh RY, Singh S, Prasad BLV, Patole MS, Sastry M, Shouche YS. 2008. Extracellular synthesis of crystalline silver nanoparticles and molecular evidence of silver resistance from *Morganella* sp.: towards understanding biochemical synthesis mechanism. *ChemBioChem* **9:** 1415-1422.
17. Pugazhenthiran N, Anandan S, Kathiravan G, Prakash NKU, Crawford S, Ashokkumar M. 2009. Microbial synthesis of silver nanoparticles by *Bacillus* sp. *J. Nanopart. Res.* **11:** 1811-1815.
18. Shahverdi AR, Minaeian S, Shahverdi HR, Jamalifar H, Nohi AA. 2007. Rapid synthesis of silver nanoparticles using culture supernatants of *Enterobacteria*: a novel biological approach. *Proc. Biochem.* **42:** 919-923.
19. Sharma VK, Yngard RA, Lin Y. 2009. Silver nanoparticles: green synthesis and their antimicrobial activities. *Adv. Colloids Interface Sci.* **145:** 83-96.
20. Sunkar S, Nachiyar CV. 2012. Biogenesis of antibacterial silver nanoparticles using the endophytic bacterium *Bacillus cereus* isolated from *Garcinia xanthochymus*. *Asian Pac. J. Trop. Biomed.* **2:** 953-959.
21. Templeton AC, Pietron JJ, Murray RW, Mulvaney P. 2000. Solvent refractive index and core charge influences on the surface plasmon absorbance of alkanethiolate monolayer-protected gold clusters. *J. Phys. Chem. B* **104:** 564-570.
22. Vaidyanathan R, Kalishwaralal K, Gopalram S, Gurunathan S. 2009. Nanosilver – the burgeoning therapeutic molecule and its green synthesis. *Biotechnol. Adv.* **27:** 924-937.
23. Zhang H, Li Q, Lu Y, Sun D, Lin X, Deng X. 2005. Biosorption and bioreduction of diamine silver complex by *Corynebacterium*. *J. Chem. Technol. Biotechnol.* **80:** 285-290.